Unravelling the mechanism of Apoptosis Induced by Copper(II) Complexes of NN_2-Pincer Ligands in Lung Cancer Cells

Athulya Das, Muniyandi Sankaralingam*

Bioinspired & Biomimetic Inorganic Chemistry Lab, Department of Chemistry, National Institute of Technology Calicut, Kozhikode-673601, Kerala, India.

*Corresponding author email: msankaralingam@nitc.ac.in; sankarjan06@gmail.com

Synthesis of Ligands (L1(H) – L4(H))

Step 1: 2-bromoacetyl bromide (1.23 g, 6.09 × 10^{-3} mol) was added dropwise to 8-aminoquinoline (0.8 g, 5.54 × 10^{-3} mol) pretreated with triethylamine (0.79 mL, 5.81 × 10^{-3} mol) in DCM (0 °C, N_2) and stirred for 30 minutes (Scheme S1). The reaction mixture was then washed with brine followed by the extraction with water and DCM. The organic fraction concentrated after filtered through celite and dried over sodium sulfate to obtain 2-bromo-*N*-(quinolin-8-yl)acetamide as a yellow crystalline powder with yield of 90(2)%.

Step 2: 2-bromo-*N*-(quinolin-8-yl)acetamide (1 g, 3.77 ×10^{-3} mol) and three equivalence (11.3 × 10^{-3} mol) of corresponding secondary amines (**L1**(H)-morpholine, **L2**(H)-diisopropylamine, **L3**(H)-dibutylamine, **L4**(H)-dibenzylamine) was dissolved in acetone and refluxed overnight. The reaction mixture was cooled and extracted using ethyl acetate followed by brine solution. The organic fraction was dried over sodium sulfate and concentrated under reduced pressure. The silica column was performed using hexane(4):ethyl acetate(1) mixture to obtain pure ligands, **L1**(H) [2-morpholino-*N*-(quinolin-8-yl)acetamide], **L2**(H) [2-di-n-propylamino-*N*-(quinolin-8-yl)acetamide], **L3**(H) [2-di-n-butylamino-*N*-(quinolin-8-yl)acetamide], **L4**(H) [2-dibenzylamino-*N*-(quinolin-8-yl)acetamide].

Isolation of copper(II) complexes 1–4

The copper(II) bromide (0.1 g, 4.47 × 10^{-4} mol) was dissolved in methanol. Then the corresponding ligand (4.47 × 10^{-4} mol) was added to the methanolic solution of copper(II) bromide at a constant stirring. Following this, triethylamine (TEA, 0.062 mL, 4.47 × 10^{-4} mol) was added to the reaction mixture. The reaction continued for 4 hrs and isolated the green coloured precipitate with cold ether and cold methanol (Scheme S1).

Scheme S1. Synthetic Route for the Present Copper(II) Complexes **1**–**3**.

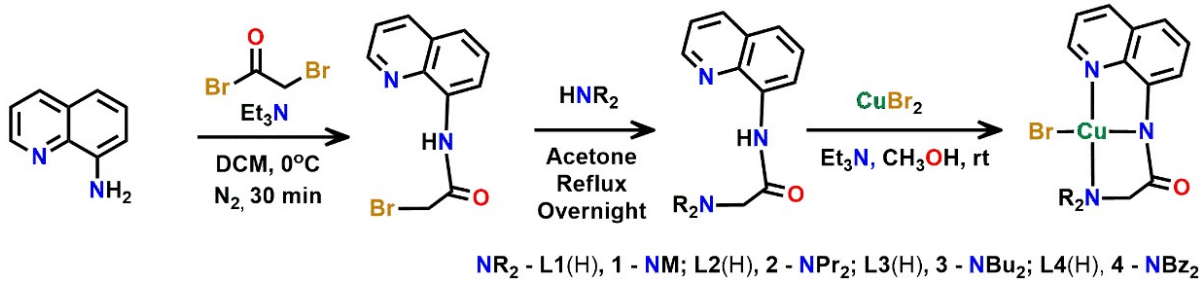

Lipophilicity

The lipophilicity of the ligands **L1**(H)–**L4**(H) and their copper complexes **1**–**4** were determined by the shake-flask method using a pre-saturated 1-octanol-water solution. Here, the partition coefficient, P (or log K_{ow}) was calculated by equation (1). In this study, water referred for, water pre-saturated with 1-octanol and octanol referrers, 1-octanol pre-saturated with water. First, 1 mg of the compound was stirred in water and the absorption of the resulting solution (A_i) using UV-visible spectroscopy was noted. This mixture was then extracted with 1-octanol and the absorption aqueous layer (A_f) was noted.

$$K_{ow} = \frac{(A_i DF_i - A_f DF_f)V_{water}}{A_f DF_f V_{octanol}} \quad (1)$$

DF_i and DF_f are the dilution factors, V_{water} and $V_{octanol}$ are the volumes of the respective fluids.

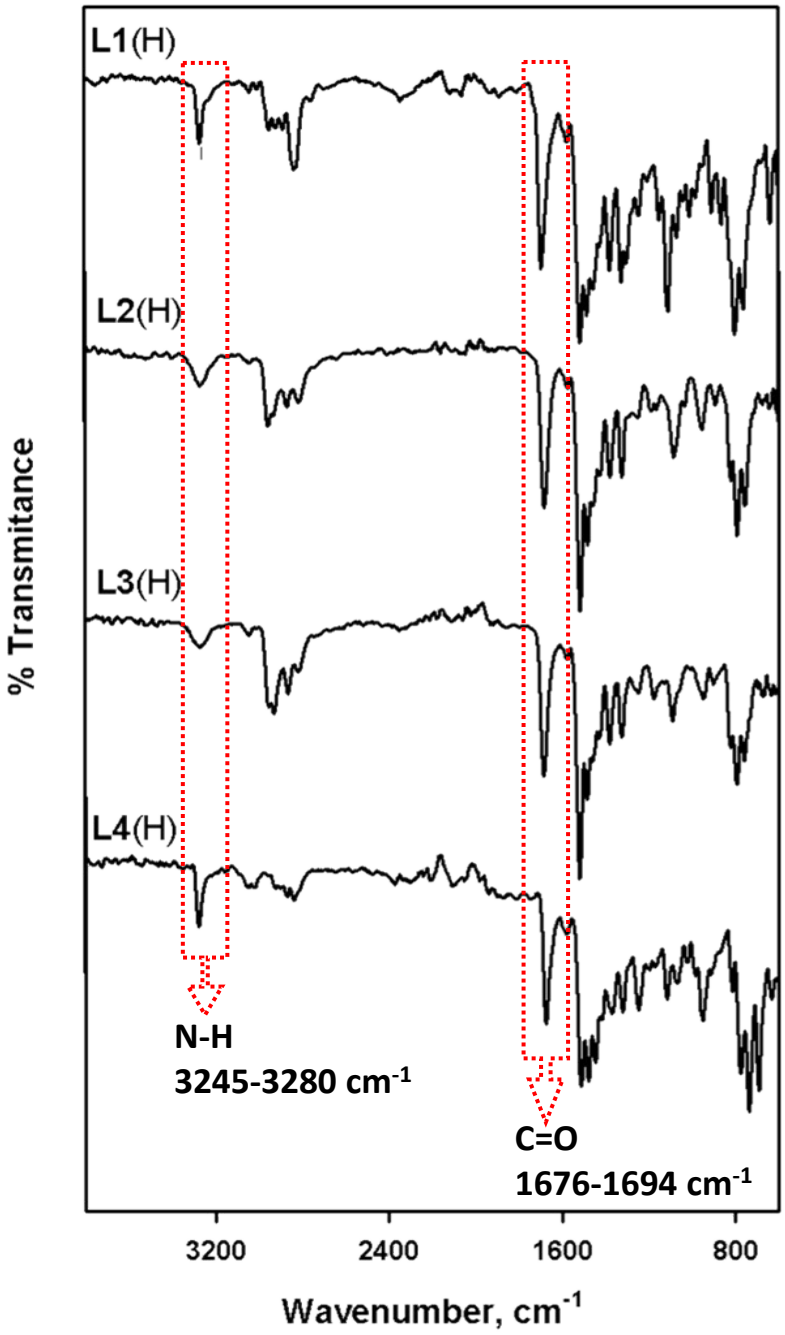

Figure S1. ATR IR spectra of **L1**(H)–**L4**(H).

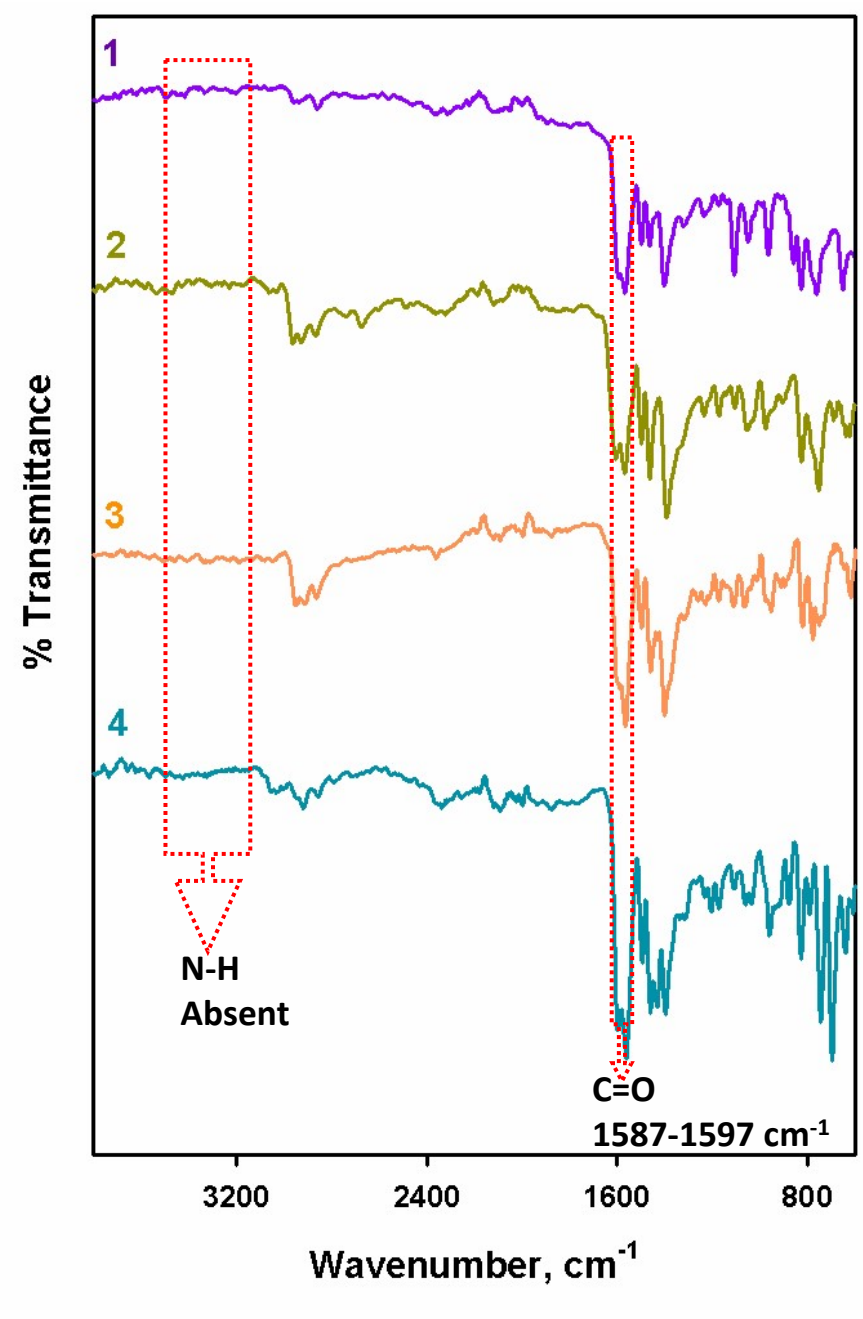

Figure S2. ATR IR spectra of **1–4**.

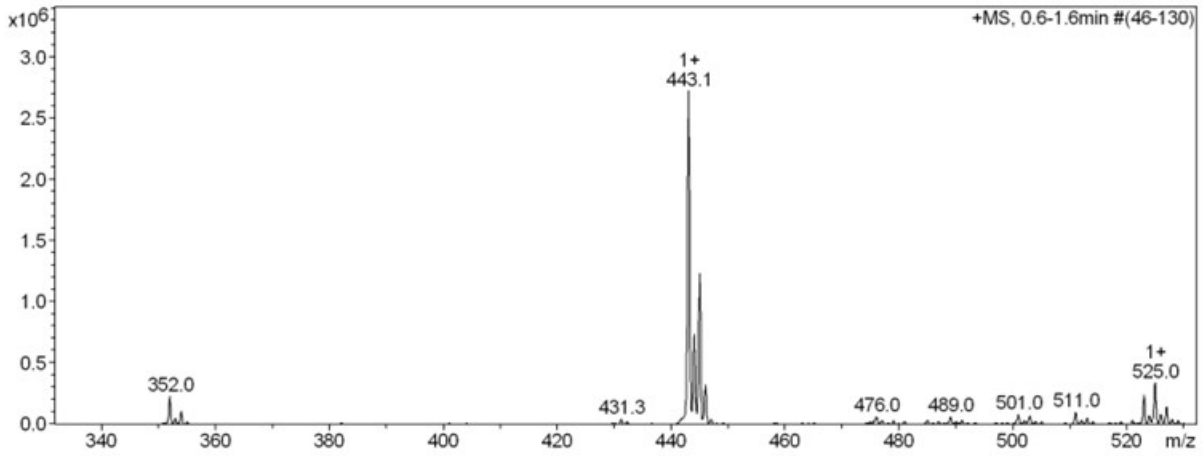

Figure S3. Mass spectrum of **4** recorded in DMSO-methanol.

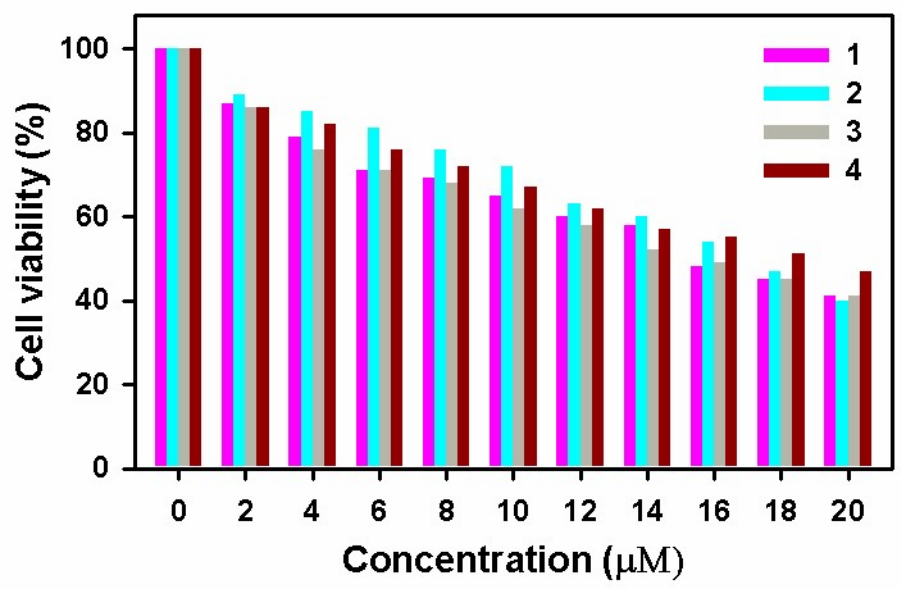

Figure S4. Percentage of cell viability of complexes **1–4** against MCF-7 cancer cell lines.

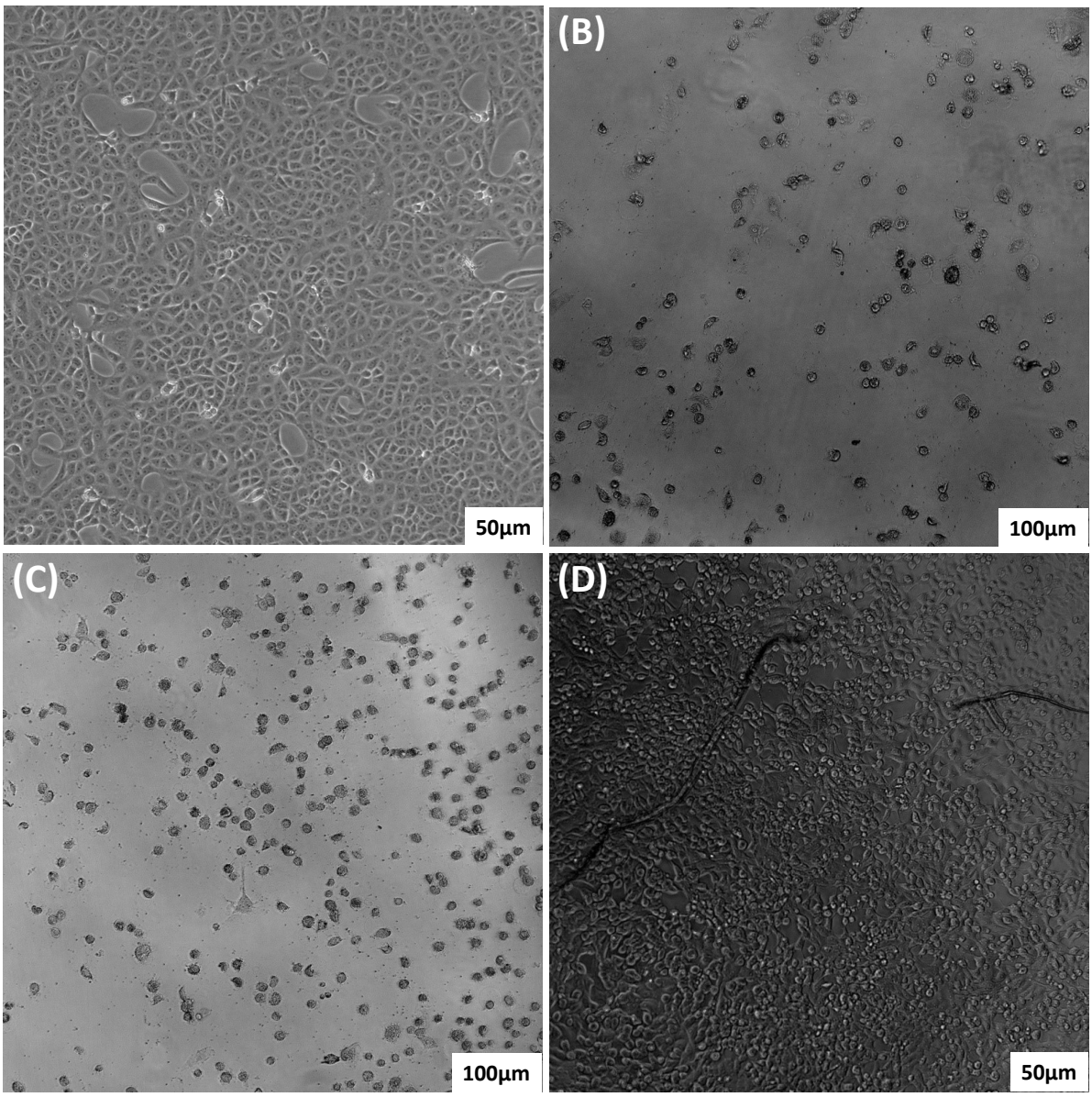

Figure S5. Phase images of (A) Control A549 cells and (B) A549 treated with **2**, (C) **3**, (D) **4**.

Table S1. Different concentrations and corresponding cell viability that obtained from MTT assay of complexes **1**–**4** against A549.

Complex 1											
Conc.(µM)	**0**	**2**	**4**	**6**	**8**	**10**	**12**	**14**	**16**	**18**	**20**
Abs. 1	1.312	0.963	0.763	0.712	0.654	0.612	0.601	0.462	0.412	0.364	0.312
Abs. 2	1.302	0.835	0.812	0.763	0.702	0.532	0.513	0.432	0.402	0.321	0.284
Abs. 3	1.336	0.867	0.795	0.725	0.626	0.602	0.524	0.502	0.423	0.402	0.364
Average	1.317	0.888	0.79	0.733	0.661	0.582	0.546	0.465	0.412	0.362	0.32
Mean	0	33	40	44	50	56	59	65	69	72	76
Viability	**100**	**67**	**60**	**56**	**50**	**44**	**41**	**35**	**31**	**28**	**24**
Complex 2											
Conc.(µM)	**0**	**2**	**4**	**6**	**8**	**10**	**12**	**14**	**16**	**18**	**20**
Abs. 1	1.326	1.102	0.945	0.912	0.845	0.812	0.745	0.684	0.624	0.602	0.462
Abs. 2	1.384	1.023	0.963	0.903	0.856	0.802	0.726	0.624	0.603	0.547	0.512
Abs. 3	1.372	1.035	0.984	0.923	0.812	0.785	0.719	0.691	0.621	0.526	0.507
Average	1.361	1.053	0.964	0.913	0.838	0.8	0.73	0.666	0.616	0.558	0.494
Mean	0	23	29	33	38	41	46	51	55	59	64
Viability	**100**	**77**	**71**	**67**	**62**	**59**	**54**	**49**	**45**	**41**	**36**
Complex 3											
Conc.(µM)	**0**	**2**	**4**	**6**	**8**	**10**	**12**	**14**	**16**	**18**	**20**
Abs. 1	1.364	1.108	0.995	0.963	0.845	0.802	0.745	0.684	0.623	0.584	0.512
Abs. 2	1.348	1.115	0.987	0.924	0.812	0.764	0.712	0.648	0.578	0.526	0.503
Abs. 3	1.387	0.998	0.992	0.934	0.863	0.823	0.802	0.624	0.614	0.523	0.522
Average	1.366	1.074	0.991	0.94	0.84	0.796	0.753	0.652	0.605	0.544	0.512
Mean	0	21	27	31	39	42	45	52	56	60	63
Viability	**100**	**79**	**73**	**69**	**61**	**58**	**55**	**48**	**44**	**40**	**37**
Complex 4											
Conc.(µM)	**0**	**2**	**4**	**6**	**8**	**10**	**12**	**14**	**16**	**18**	**20**
Abs. 1	1.346	1.299	1.154	1.154	1.113	0.972	0.896	0.812	0.728	0.688	0.629
Abs. 2	1.325	1.195	1.128	1.123	0.982	0.913	0.862	0.847	0.755	0.693	0.566
Abs. 3	1.229	1.186	1.103	0.998	0.934	0.888	0.846	0.824	0.802	0.768	0.744
Average	1.3	1.227	1.128	1.092	1.01	0.924	0.868	0.828	0.762	0.716	0.646
Mean	0	6	13	16	22	29	33	36	41	45	50
Viability	**100**	**94**	**87**	**84**	**78**	**71**	**67**	**64**	**59**	**55**	**50**

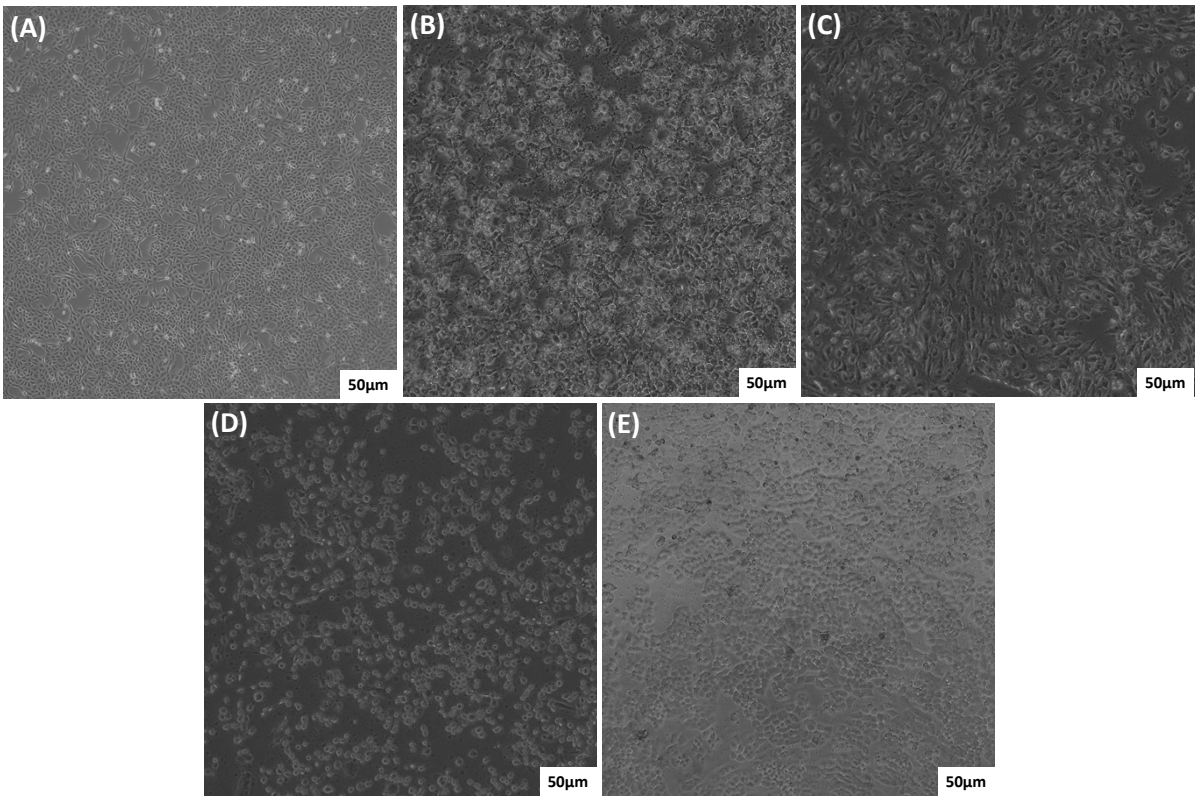

Figure S6. Phase images of (A) control MCF-7 cells and (B) MCF-7 treated with **1**, (C) **2** (D) **3**, (E) **4**.

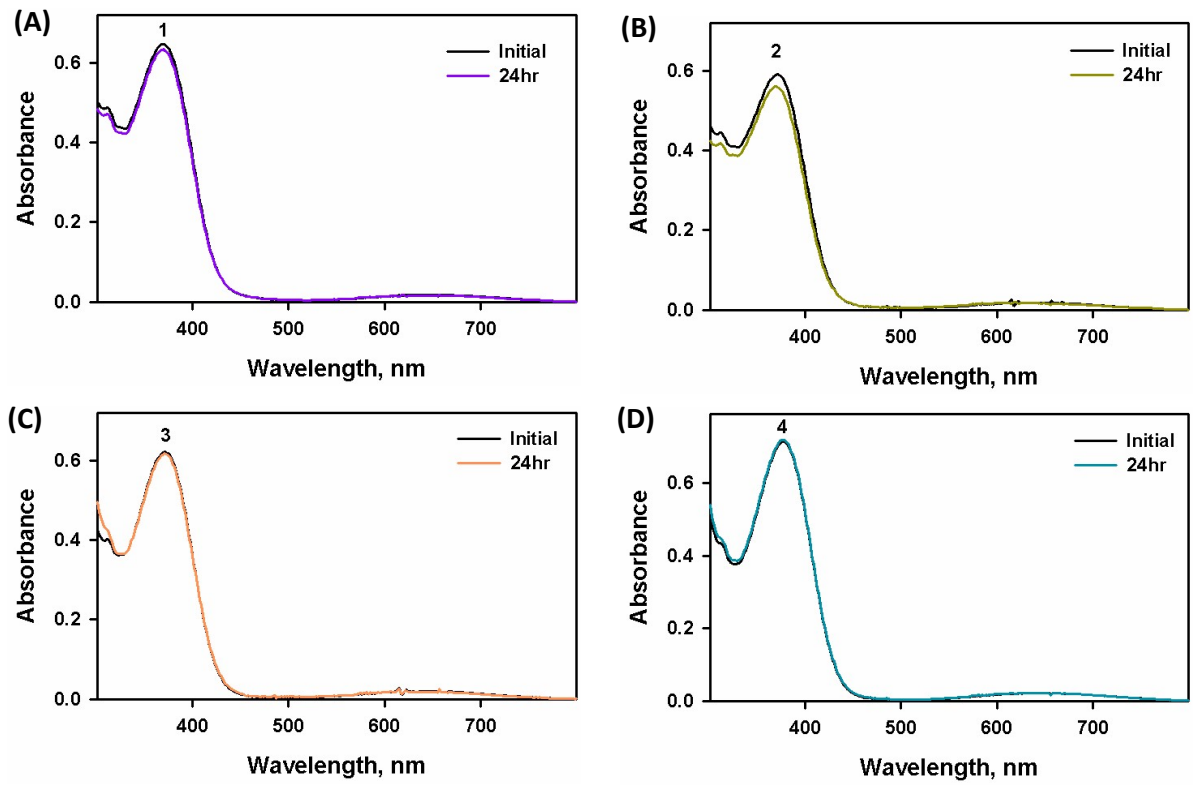

Figure S7. UV-vis spectra of complexes (A (**1**), B (**2**), C(**3**) and D(**4**)) were recorded in DMSO at a time interval of 24h.

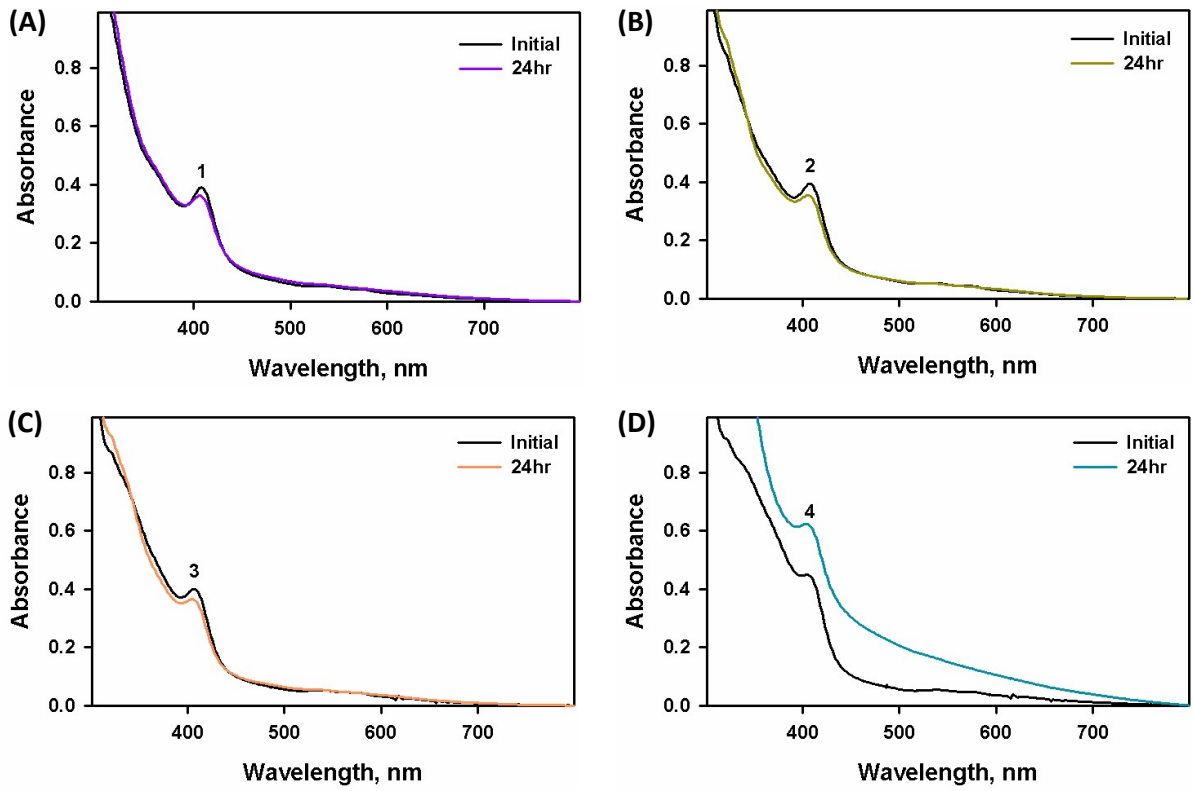

Figure S8. UV-vis spectra of complexes ((A (**1**), B (**2**), C (**3**) and D(**4**))) were recorded in FBS at a time interval of 24 h.

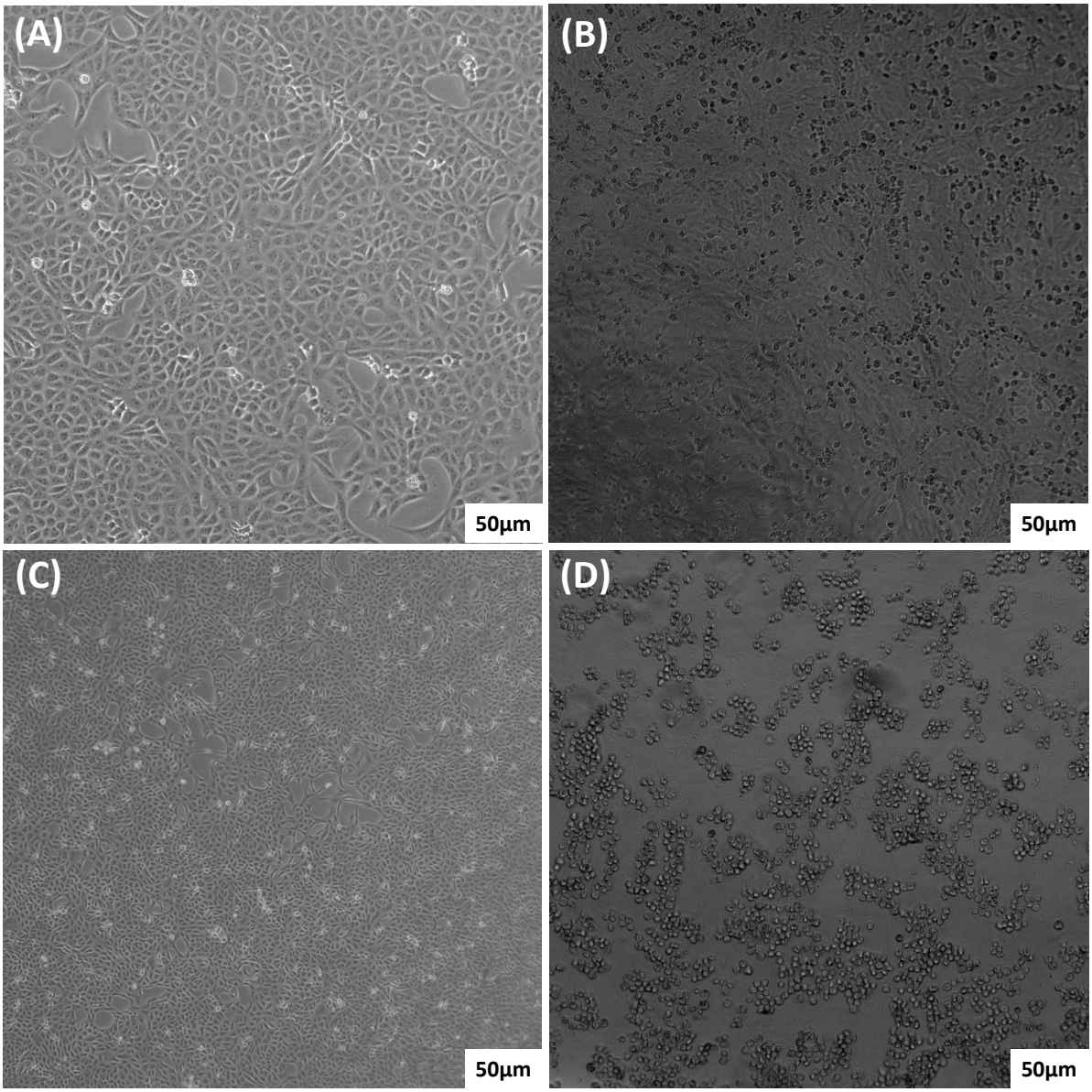

Figure S9. Phase images of (A) control A549 cells and (B) A549 treated with **L1**(H), (C) control MCF-7 cells (D) MCF-7 cells treated with **L1**(H).

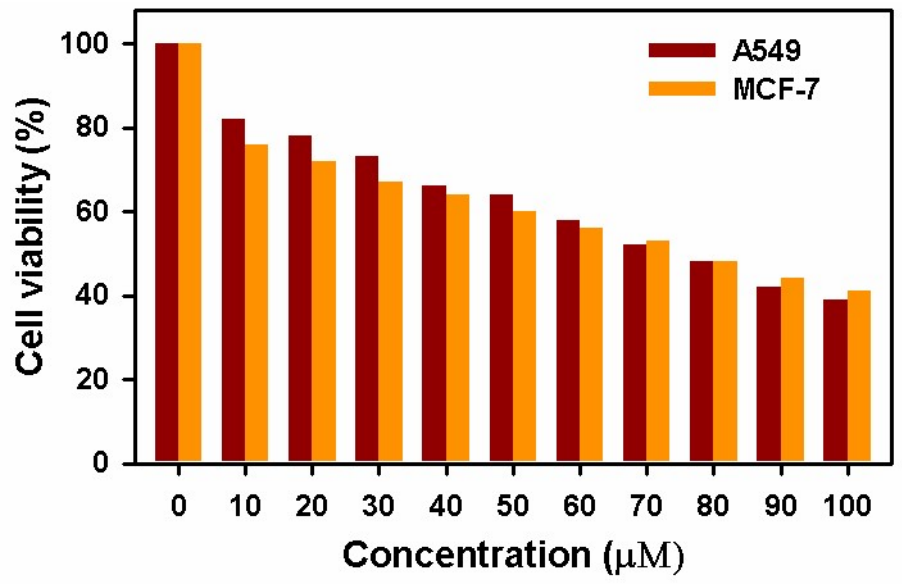

Figure S10. Percentage of cell viability of ligand **L1**(H) against A549 and MCF-7 cancer cell lines.

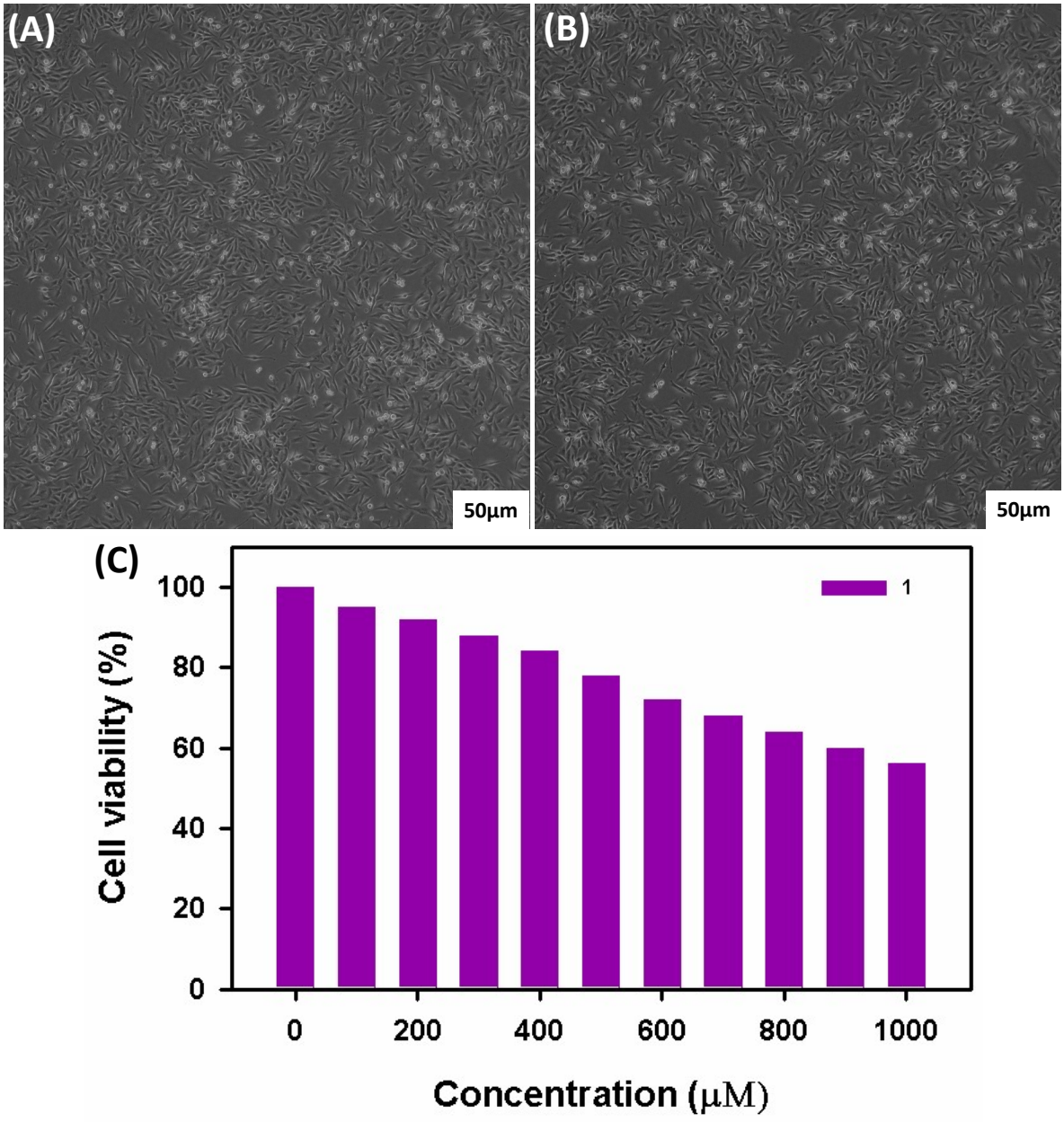

Figure S11. Phase images of (A) control L929 cells and (B) L929 treated with **1**, (C) percentage of cell viability of **1** against L929 cells.

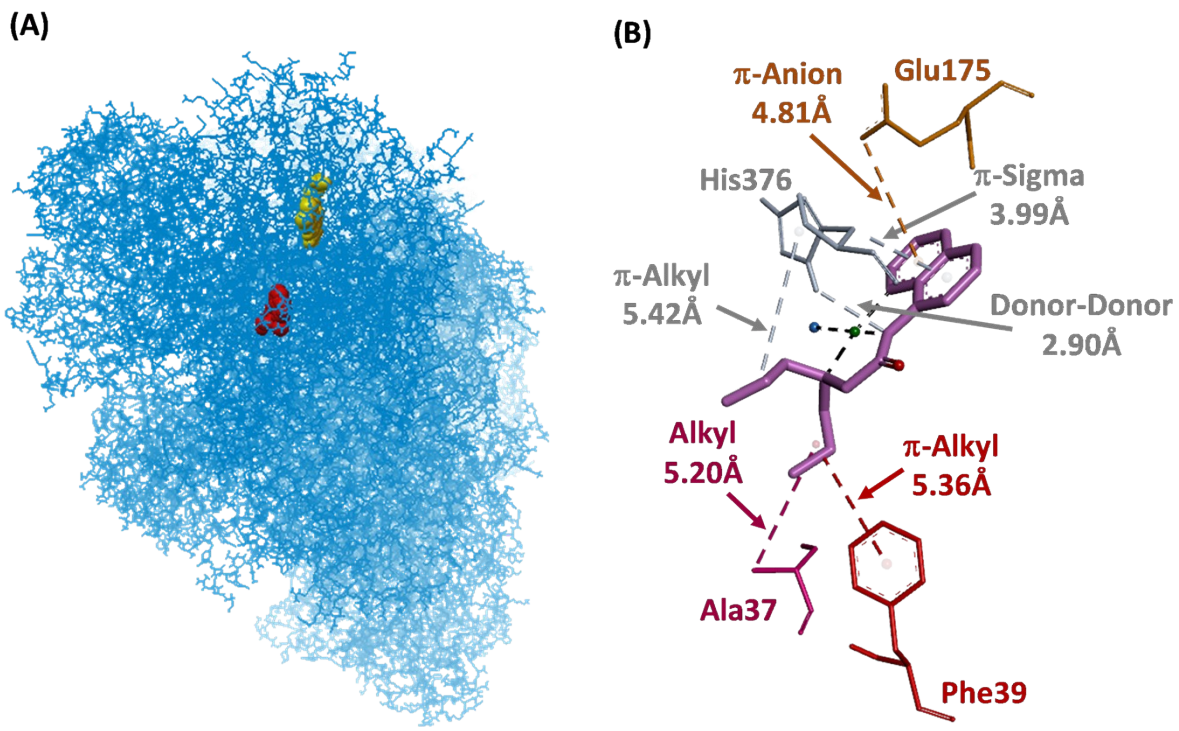

Figure S12. (A) Molecular docked conformation and (B) interactions of **2** in the active site of 5XTD.

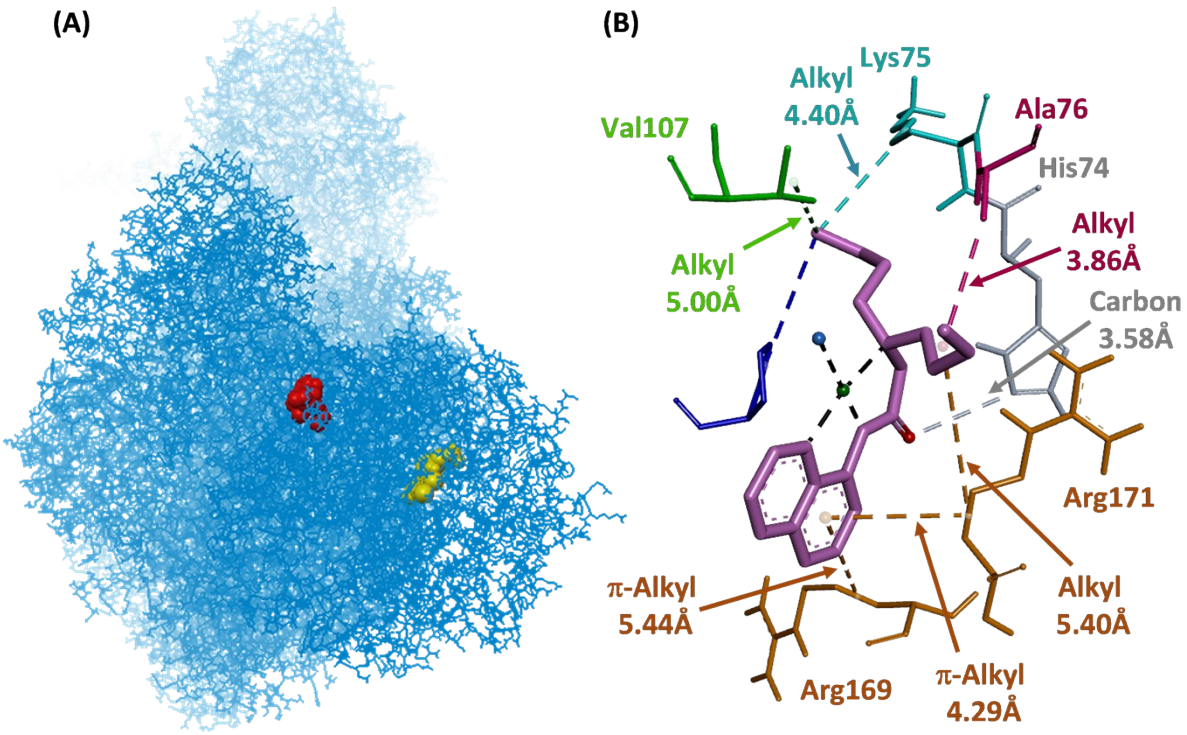

Figure S13. (A) Molecular docked conformation and (B) interactions of **3** in the active site of 5XTD.

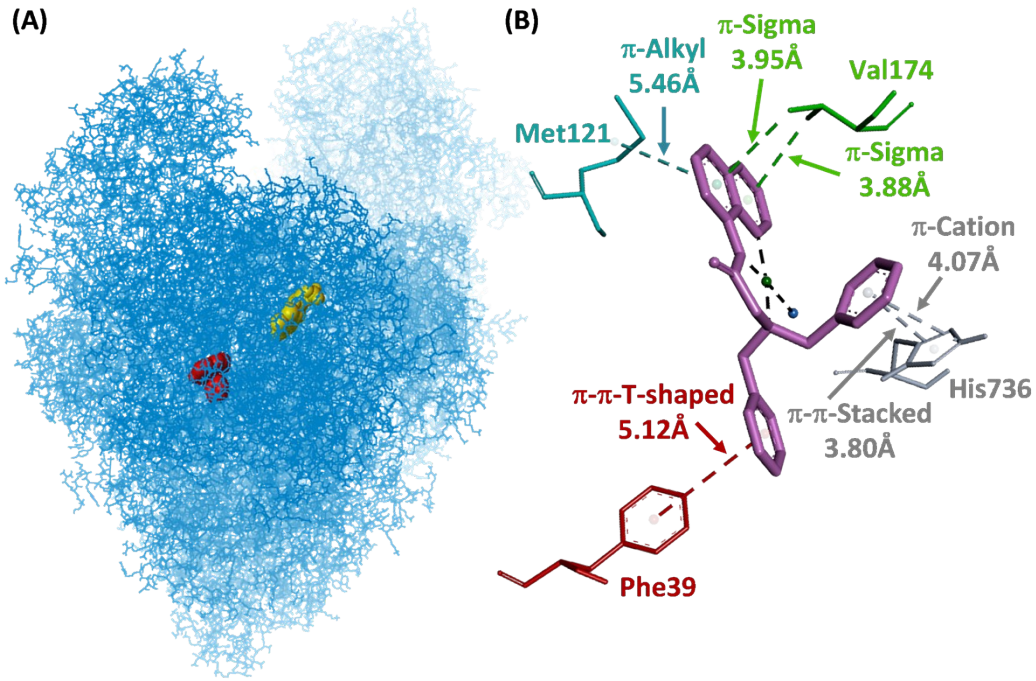

Figure S14. (A) Molecular docked conformation and (B) interactions of **4** in the active site of 5XTD.

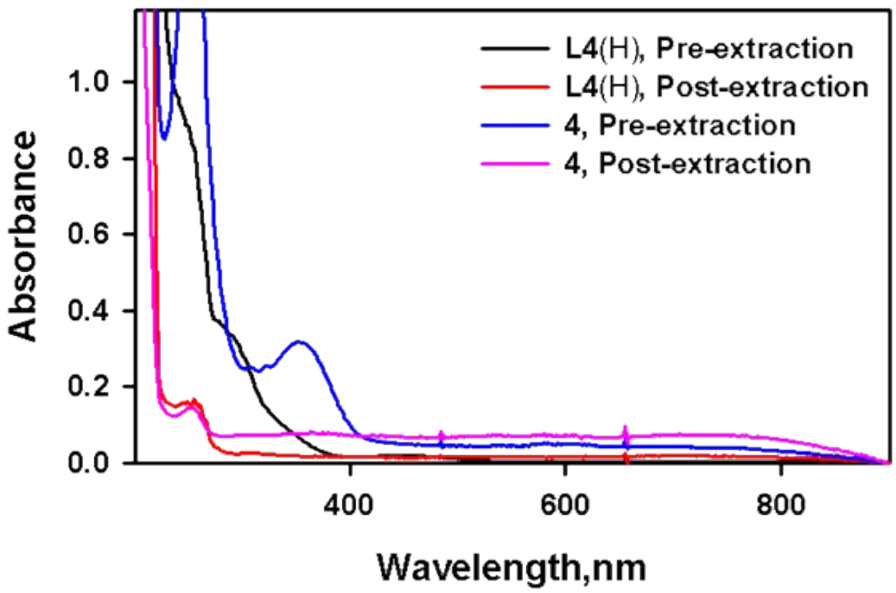

Figure S15. UV-visible spectra of **L4**(H) (black and red) and **4** (Blue and pink) in aqueous phase before (black and blue) and after (red and pink) extraction with the water-saturated 1-octanol.

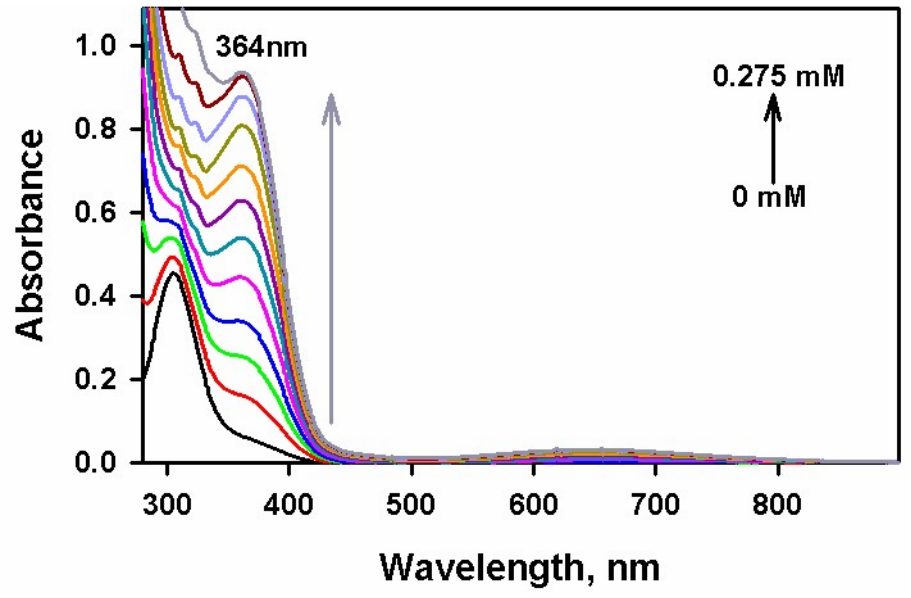

Figure S16. Changes observed in UV-visible absorption spectra during the reaction of a fixed concentration (0.25 mM) of $CuBr_2$ with an incremental addition (0.025 mM) of 2-di-n-benzylamino-*N*-(quinolin-8-yl)acetamide up to 0.275 mM in methanol.